Use of Monitoring Data to Update Performance Predictions of Supported Excavations

Richard J. Finno[1] M. ASCE, P.E.

[1]Professor, Department of Civil and Environmental Engineering, Northwestern University, Evanston, Il. 60208, r-finno@northwestern.edu

ABSTRACT: Successful use of monitoring data to update performance predictions of supported excavations depends equally on reasonable numerical simulations of performance, the type of monitoring data used as observations, and the inverse analysis techniques used to minimize the difference between predictions and observed performance. This paper summarizes each of these factors and emphasizes their inter-dependence. Numerical considerations are described, including the selection of the type of finite element formulation, the initial stress conditions with emphasis on urban environments, the importance a reasonable representation of the construction process, and factors affecting the selection of the constitutive model. Monitoring data that can be used in conjunction with current numerical capabilities are discussed and a gradient-based inverse analyses technique that has been successfully used to update predictions of lateral ground movements measured close to support walls is summarized. Examples from application of these techniques from case studies are presented to illustrate the capabilities of this approach.

INTRODUCTION

Many factors affect the ground movements caused by excavations, including stratigraphy, soil properties, support system details, construction activities, contractual arrangements and workmanship. While numerical simulations have become more common to analyze ground response to excavations as part of the design process, finite element predictions contain uncertainties related to soil properties, support system details, and construction procedures. If one wants to predict and subsequently evaluate the overall performance of a design, a procedure that incorporates an evaluation of the results of the predictive analysis must be defined. The procedure to accomplish this task is usually referred to as the "observational method" (Peck, 1969), a framework wherein construction and design

procedures and details are adjusted based upon observations and measurements made as construction proceeds. While the observational method is conceptually very helpful, it is quite difficult to use observed movements for controlling construction in a timely enough fashion to be of use in a typical excavation project, where time is of the essence to a contractor, or to judge quantitatively how well the work is proceeding. Recent developments in sensor technology, information technology and numerical analysis conceptually allow one to automate the cycle of measurement and prediction update based on observed performance.

This paper summarizes the state of the practice of using inverse analysis techniques to minimize the difference between computed and observed excavation performance data. The goal of such analyses is to allow one to use the observed performance at early stages of a project to objectively calibrate a predictive model so that predictions of subsequent performance can be made more confidently. The successful application of such techniques depends on the predictive model, in this case a finite element simulation of construction, the monitoring data and the inverse technique itself. This paper will illustrate these points by examining the technique as applied to supported excavations made through soft to medium clays. Comments are made regarding how details of the finite element simulations, the instrumentation and data collection, and the inverse technique affect the results of the methodology. Several examples of excavations where these techniques were applied are presented.

The approach taken herein is one of parameter estimation based on minimizing the difference between computed results and field observations. Thus it is assumed that the stratigraphy and the construction procedures are known. This is clearly an approximation, especially in the design phase of a project. However, the flexibility of the method will allow one to modify the construction procedure based on actual events as the project progresses. Material variability is not explicitly included, but the optimized parameters are taken to be the average within a particular stratum.

FINITE ELEMENT PREDICTIONS OF EXCAVATION PERFORMANCE

A key to a successful finite element simulation is to reasonably represent within a numerical simulation pertinent field activities during construction. In addition to replicating construction procedures, there are several other important factors that have an impact on the computed responses - including the constitutive model, dimensionality of the problem, and initial ground stresses – and these must be considered when evaluating results of the update procedure.

Construction Process

While supported excavations commonly are simulated numerically by modeling cycles of excavation and support installation, it is necessary to simulate all aspects of the construction process that affect the stress conditions around the cut to obtain an accurate prediction of behavior. This may involve simulating previous construction activities at the site, installation of the supporting wall and any deep foundation elements, as well as the removal of cross-lot supports or detensioning of tiedback

ground anchors. Furthermore, issues of time effects caused by hydrodynamic effects or material responses may be important.

Drainage Conditions

An important preliminary decision in any analysis is to match the expected field drainage conditions, which impacts the formulation required. Clough and Mana (1976) and field data have shown that for excavations through saturated clays with typical excavation periods of several months, the clays remain essentially undrained with little dissipation of excess pore pressures. However, there may be cases (i.e., O'Rourke and O'Donnell 1997) where substantial delays during construction occur and excess pore pressures partially dissipate, and in these cases one must use a mixed formulation to account for the pore water effects.

For undrained conditions, one can employ either a coupled finite element formulation where both displacements and pore water pressures are solved for explicitly (e.g. Carter et al. 1979) or a penalty formulation (e.g. Hughes 1980) wherein the bulk modulus of water – or a sufficiently large number that depends on the precision of the machine making the computation - is added to the diagonal terms in the element stiffness matrix during global matrix assembly. This additional term constrains the volumetric strain to nearly zero, i.e., undrained. In both these approaches, the constitutive response of the soil is defined in terms of effective stress parameters.

A simpler, alternate approach is to define the constitutive response in terms of total stress parameters, with care being taken to make the diagonal terms of the element stiffness matrix large, typically by using a Poisson's ratio close to 0.5. In this case, a Young's modulus corresponds to an undrained value and failure is expressed in terms of an undrained shear strength, Su (e.g., $\varphi = 0$ and $c = Su$).

Initial Conditions

A reasonable prediction of the ground response to construction of a deep excavation starts with a good estimate of the initial stress conditions, in terms of both effective stresses and pore water pressures. The effective stress conditions for excavations in well-developed urban areas rarely correspond to at-rest conditions because of the myriad past uses of the land. Existence of deep foundations and/or basements from abandoned buildings and nearby tunnels changes the effective stresses from at-rest conditions prior to the start of excavation. For example, Calvello and Finno (2003) showed that an accurate computation of movements associated with an excavation could only be achieved when all the pre-excavation activities affecting the site were modeled explicitly. They used the case of the excavation for the Chicago-State subway renovation project (Finno et al. 2002). In this project, construction of both a tunnel and a school impacted the ground stresses prior to the subway renovation project. Ignoring these effects made a difference of a factor of 3 in the computed lateral movements.

One must also take care when defining the initial ground water conditions. Even in cases where the ground water level is not affected by near surface construction

activities, non-hydrostatic conditions can exist for a variety of reasons. For example, Finno et al. (1989) presented pneumatic piezometer data that indicated a downward gradient within a 20 m thick sequence of saturated clays. This downward flow arose from a gradual lowering of the water level in the upper rock aquifer in the Chicago area since the 1950s. A non-hydrostatic water condition affects the magnitude of the effective stresses at the start of an excavation project.

An engineer has two choices to define such conditions – to measure the *in situ* conditions directly or to simulate all the past construction activities at a site starting from appropriate at-rest conditions. Because both approaches present challenges in their own right, it is advantageous to do both to provide some redundancy in the input. In any case, careful evaluation of the initial conditions is required when numerically simulating supported excavation projects, especially in urban areas.

Wall Installation

Many times the effects of the installation of a wall are ignored in a finite element simulation and the wall is "wished-into-place" with no change in the stress conditions in the ground or any attendant ground movements. However, there is abundant information that shows ground movements may arise during installation of the wall.

O'Rourke and Clough (1990) present data that summarize observed settlements that developed during installation of 5 diaphragm walls. They noted settlements as large as 0.12% of the depth of the trench. These effects can be evaluated by 3-dimensional modeling of the construction process (e.g., Gourvenec and Powrie 1999), but not without several caveats. The specific gravity of the supporting fluid usually varies during excavation of a panel as a result of excavated solids becoming suspended – increasing the specific gravity above the value of the water and bentonite mixture – and subsequently decreasing when the slurry is cleaned prior to the concrete being tremied into place. Consequently, it is difficult to select one value that represents an average condition. Furthermore the effects of the fluid concrete on the stresses in the surrounding soil depend how fast the concrete hardens relative to its placement rate. Some guidance in selecting the fresh concrete pressure is provided by Lings et al. (1994).

It is less straightforward when modeling diaphragm wall installation effects in a plane strain analysis because the arching caused by the excavation of individual panels cannot be taken directly into account. To approximate the effects of the arching when making such an analysis, an equivalent fluid pressure must be applied to the walls of the trench to maintain stability that is generally higher than the level of the fluid during construction. Thus, some degree of empiricism is required to consider these effects in plane strain analyses. One can back-calculate an equivalent fluid pressure corresponding to the observed ground response if good records of lateral movements close to the wall are recorded during construction. More data of this type are needed before any recommendations can be made regarding magnitudes of appropriate equivalent pressures.

The effects of installing a sheet pile wall are different than those of a diaphragm wall, yet the effects on observed responses also can be significant. In this case, ground movements may arise from transient vibrations developed as the sheeting is

driven or vibrated into place and ground movements from the physical displacement of the ground by the piles. The former mechanism is of practical importance if installing the piles through loose to medium dense sands, and can be estimated by procedures proposed by Clough et al. (1989). However, these effects are not included in finite element simulations. The latter mechanism in clays was illustrated by Finno et al. (1988). In this case, the soil was displaced away from the sheeting as it was installed and was accompanied by an increase in pore water pressure and a ground surface heave. As these excess pore water pressures dissipated, the ground settled. The maximum lateral movement and surface heave was equal to one-half the equivalent width of the sheet pile wall, defined as the cross-sectional area of the sheet pile section per unit length of wall. Sheet-pile installation can be simulated in plane strain by using procedures summarized in Finno and Tu (2006).

In addition to the movements that occur as a wall is installed, installing the walls can have a large influence on subsequent movements, especially if the walls are installed relatively close to each other, as may be the case in cut-and-cover excavation for a tunnel. Sabatini (1991) conducted a parametric study as a function of the depth, H, to width, B, of the excavation, wherein the effects of sheet-pile wall installation in clays were compared with simulations where the walls were wished into place. The results of the study are shown in Figure 1 where the computed normalized maximum lateral movements, $\delta H_{(max)}$, are plotted versus H/B. It is apparent for wide excavations (H/B $\leq$ 0.25) that the decision to include installation effects in a simulation is not critical. However, these effects become pronounced for narrow excavations (H/B » 1) and should be explicitly considered. The results show that for the "wished-in-place" case when the sheet-pile installation effects are ignored, the lateral movements are larger for wider excavations, a similar trend reported by Mana and Clough (1981).
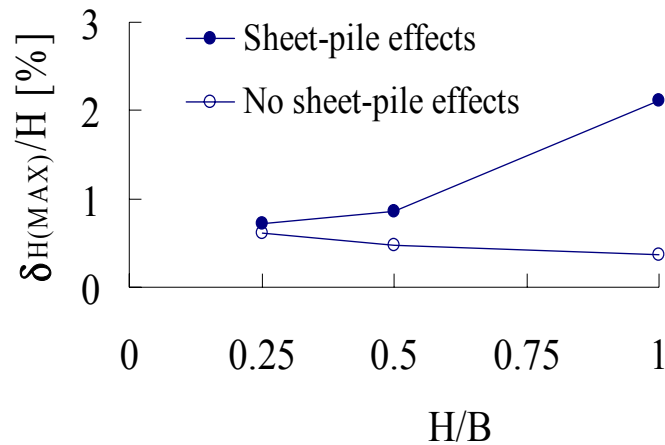
Fig. 1. Effects of sheet-pile installation on computed lateral movements

The installation procedure has two main effects: the soil adjacent to the excavation is preloaded and the shear strength on the passive side is (partially) mobilized prior to the beginning of the cycles of excavation. Wall installation tends to preload the soil on the active side of the excavation as a result of the reduction in shear stress at approximately constant mean normal effective stress. This mechanism provides the

soil outside the walls with more available shearing resistance when the cycles of excavation start. However, the soil between the walls has less available passive resistance as a result of the preloading and this promotes the larger movements during excavation as compared to the case of ignoring the sheet-pile effects (Finno and Nerby 1989).

Excavation And Support Cycles

Ghaboussi and Pecknold (1985) indicated that the correct solution to the incremental excavation problem involves satisfying at any step *n*:

$$R_{(n)} = F_{ext(n)} - F_{int(n)} = \int_{\Omega^e} \gamma_t N^T f d\Omega^e - \int_{\Omega^e} B^T \sigma d\Omega^e$$

(1)

where *R* is the residual force vector, F_{ext} is the external force vector, F_{int} is the internal force vector, γ_t is the total unit weight of the soil, *N* is the shape function matrix, *f* is the unit body force vector, Ωe is the element domain, *B* is the strain-displacement matrix, σ is the vector of total stresses and the superscript *T* implies a matrix transposition. For equilibrium R equals zero. In (1), the total gravity loads are balanced by total internal stresses distributed over the excavated surface. Equation (1) implies that whenever water is present and the constitutive response is represented by an effective stress model, both total and effective stress vectors must be saved. Other approaches for simulating the excavation process (e.g. Christian and Wong 1973) are approximate and can lead to errors in the solution simply as a result of applying incorrect loads.

    Care must be taken when specifying water levels in conjunction with excavation loading. In some cases, the physics of the solution removes any potential ambiguity when handling the water levels. For example, for excavations through high permeability soils, the excavation must be dewatered prior to removing the soil in the field and the water levels in the numerical simulation must represent the dewatered state. In contrast, when excavating through saturated clays wherein the constitutive responses are represented by an effective stress model, one must be sure that the σ in (1) is indeed total stresses and that the water levels are correctly manipulated throughout the simulation. If a mixed formulation is used, the phreatic surface inside the excavation must be specified as the excavated surface, but ideally there should be small enough elements so sharp gradients can exist near the excavated surface and little dissipation of excess pore water pressure occurs during the normal durations of excavations. Commercially available codes handle the question of pore water pressures and excavation forces in various ways, and thus excavation procedures vary from code to code.

Representing Structural Support Elements

    Representing lateral support elements in a finite element simulation in plane strain conditions is accomplished by dividing the actual support stiffness by the support spacing. For cross lot bracing, this is a direct procedure. In this case, the effect of the waler is assumed to uniformly spread the load to the wall. When a wall is supported

by tiebacks, several options are available to an analyst. One can model the ground anchor and the tie rod explicitly, thereby resulting in a relatively complicated mesh. The ground anchor can be represented as a solid element surrounded by interface elements and the tie rod can be represented by a bar element tied to the wall and the end of the ground anchor. The benefits of going to these extremes are not necessarily clear, given the simplifications inherent in the model, e.g., the effects of drilling and grouting pressures are not included in the analysis. Clough and Tsui (1974) suggested that the tiebacks could be represented by bar elements attached to the wall oriented along the line of the tieback with its stiffness equal to the tie rod stiffness divided by its spacing. In this simplified approach, it is assumed that the ground anchor is unyielding. If performance test data are available, one can use the stiffness determined from the unloading portion of the test from the maximum load to the lock-off load.

Sometimes it is necessary to model tieback anchors in a particular way because of the geometry of the installation. Figure 2 shows a section of the support system for the Lurie Center excavation (Finno and Roboski 2005). The top two rows of ground anchors were supported in the same sand stratum. The horizontal spacing between the anchors was 1.5 m, but the anchors at levels 1 and 2 were staggered so that there was nominally at least 0.75 m between each anchor. When making a plane strain analysis of this excavation, if one explicitly models the entire anchor, there will be very little space between the two rows of anchors.
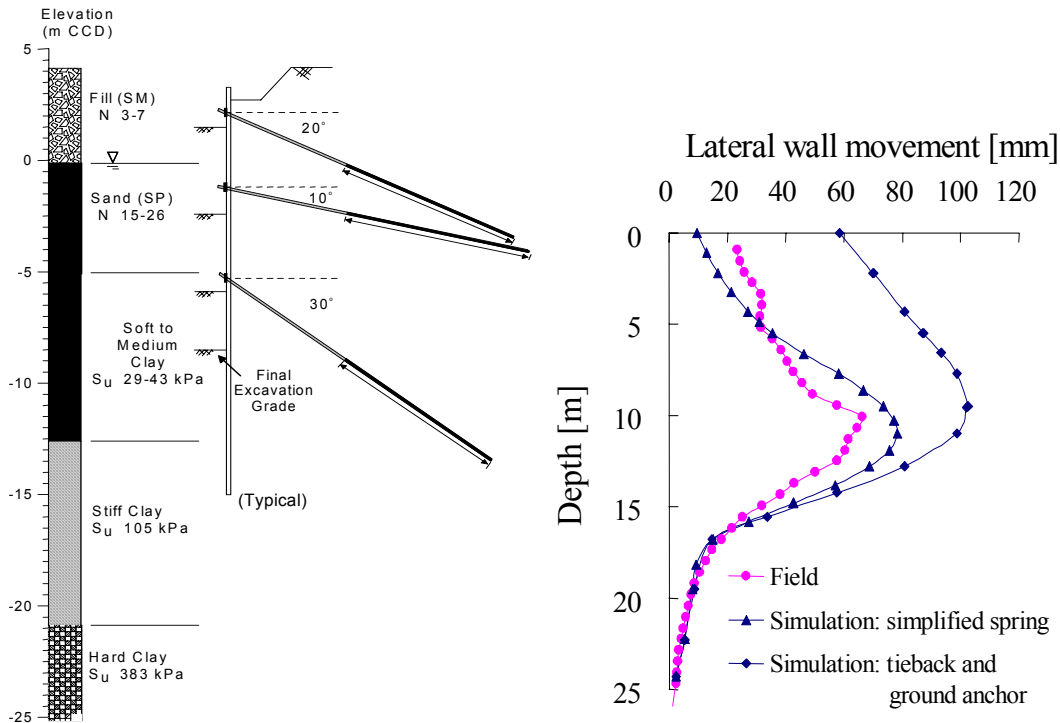
Fig. 2. Effect of tieback FE representation at Lurie excavation

To illustrate the effect this can have on computed displacements, Figure 2 also shows horizontal displacements computed by considered the anchor system explicitly

7

and the simplified approach. The simulation was made with ABAQUS and the same soil parameters were used in each simulation. Also shown is inclinometer data obtained at the end of the excavation. The more complicated approach produces much higher lateral displacements form of a rotation of the displaced profile, as a result of movements of the ground anchors. This is not observed in the computed results for the simplified approach, which better reproduced the observed movements. This admittedly is an extreme case because of the proximity of the two upper levels of the ground anchors. The finite element discretization near the end of the ground anchors was such that only one row of soil elements were located between the anchors, exaggerating the effects of the load transfer from the anchors to the soil, and resulting in excessive lateral movements near the top of the wall.

Plane Strain versus 3-Dimensional Analyses

Figure 3 illustrates some of the challenges of using field observations to calibrate numerical models of any kind, even when detailed records exist. This figure summarizes the construction progress at the Chicago-State excavation in terms of excavation surface and support installation on one of the walls of the excavation for selected days after construction started. Also shown are the locations of two inclinometers placed several meters behind the wall. If one is making a computation assuming plane strain conditions, then it is clear that one must judiciously select a data set so that planar conditions would be applicable to a set of inclinometer data. If one is using an integrated approach wherein data is collected and compared with numerical predictions in almost real time, then it is clear that a 3D analysis would be required for most days as a result of the uneven excavated surface and timing of the anchor prestressing operations.
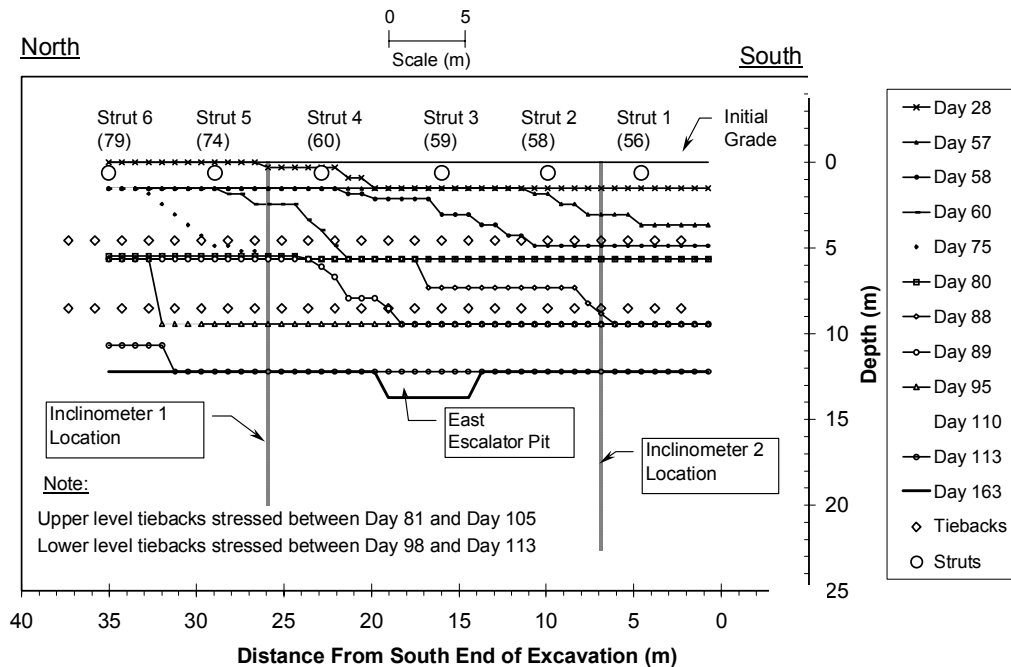
Fig. 3. Construction progress at excavation in Chicago (Finno et al 2002)

8

Even when a sufficiently extensive horizontal excavated surface is identified, 3-dimensional effects may still arise from the higher stiffness at the corners of an excavation. These boundary conditions lead to smaller ground movements near the corners and larger ground movements towards the middle of the excavation wall. Another, and less recognized, consequence of the corner stiffening effects is the maximum movement near the center of an excavation wall may not correspond to that found from a conventional plane strain simulation of the excavation, i.e., 3-dimensional (3-D) and plane strain simulations of the excavation do not yield the same movement at the center portion of the excavation, even if the movements in the center are perpendicular to the wall (Ou et al. 1996). This affect can be quantified by the plane strain ratio, PSR, defined herein as the maximum movement in the center of an excavation wall computed by 3-D analyses divided by that computed by a plane strain simulation. Finno et al. (2007) developed the following expression for PSR from the results of a finite element parametric study of excavations through clay:

$$PSR = \left(1 - e^{-k\,C(L/H_e)}\right) + 0.05\left(L/B - 1\right) \qquad (2)$$

where L is the length of the excavation where the movement occurs, B is the other areal dimension, and H_e is the excavation depth. The value of C depends on the factor of safety against basal heave, FS_{BH}, and is taken as:

$$C = 1 - \left\{0.5\,(1.8 - FS_{BH})\right\} \qquad (3)$$

The value of k depends on the support system stiffness, S, and is taken as:

$$k = 1 - 0.0001\left(\frac{EI}{\gamma h^4}\right) \qquad (4)$$

where EI is the bending stiffness of the wall, γ is the total unit weight of the soil and h is the average vertical spacing between supports. When L/H_e is greater than 6, the PSR is equal to 1 and results of plane strain simulations yield the same displacements in the center of an excavation as those computed by a 3-D simulation. When L/H_e is less than 6, the displacement computed from the results of a plane strain analysis will be larger than that from a 3-D analysis. When conducting an inverse analysis of an excavation with a plane strain simulation, the effects of this corner stiffening is that an optimized stiffness parameter will be larger than it really is because of the lack of the corner stiffening in the plane strain analysis. This effect becomes greater as an excavation is deepened because the L/H_e value increases as the excavated grade is lowered. This trend was observed in the optimized parameters for the deeper strata at the Chicago-State subway renovation excavation (Finno and Calvello 2005).

Constitutive Models

When one undertakes a numerical simulation of a deep supported excavation, one of the key decisions made early in the process is the selection of the constitutive model.

In general, this selection should be compatible with the objectives of the analysis. If the results form the basis of a prediction that will be updated based on field performance data, then the types of field data that form the basis of the comparison will impact the applicability of a particular model. Possibilities include lateral movements based on inclinometers, vertical movements at various depths and distances from an excavation wall and/or forces in structural support elements. When used for a case where control of ground movements is a key design consideration, the constitutive model must be able to reproduce the soil response at appropriate strain levels to the imposed loadings.

It is useful to recognize that soil is an incrementally nonlinear material, i.e., its stiffness depends on loading direction and strain level. Real soils are neither linear elastic nor elastic-plastic, but exhibit complex behavior characterized by zones of high constant stiffness at very small strains, followed by decreasing stiffness with increasing strain. This behavior under static loading initially was realized through back-analysis of foundation and excavation movements in the United Kingdom (Burland, 1989). The recognition of zones of high initial stiffness under typical field conditions was followed by efforts to measure this ubiquitous behavior in the laboratory for various types of soil (Jardine et al, 1984; Clayton and Heymann 2001; Santagata et al. 2005; Callisto and Calebresi 1998, Holman 2005, Cho 2007).

To illustrate this behavior, Figure 4 shows the results of drained, triaxial stress probes conducted on specimens cut from block samples obtained at an excavation in Evanston, IL. Each specimen was reconsolidated under K_0 conditions to the in-situ vertical effective stress σ_{v0}', maintained a 36 hour K_0 creep cycle, and then subjected to directional stress probes under drained axisymmetric conditions. Bender element (BE) tests were conducted during the reconsolidation and stress probing portions of the test for each specimen.
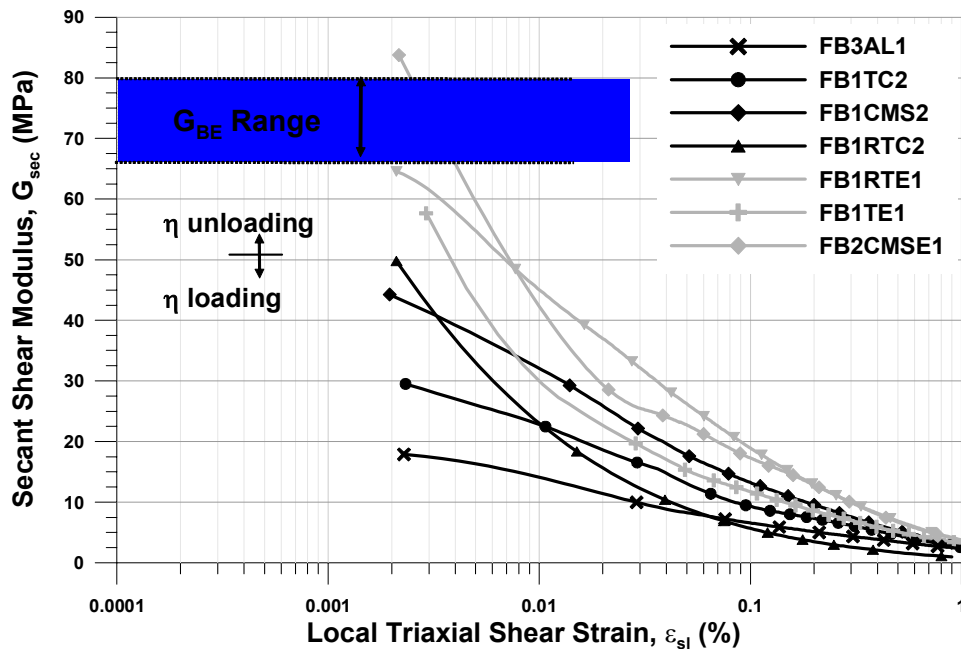
Fig. 4. Secant shear modulus as a function of direction of loading

The secant shear modulus was plotted versus triaxial shear strain in Figure 4 for natural specimens whose stress probes involved changes in the shear stress q. The overconsolidation ratio of these specimens was 1.7, so if one assumes the response is isotropic and elasto-plastic, then G should be constant. The stress probes wherein q and the stress ratio, $\eta = q/p'$, is increased ("η loading") are clearly softer than those where q and η initially decrease ("η unloading). There are no obvious zones of constant G_{sec} at shear strains greater than 0.002%, and thus no elastic zone is observed in these data for strain levels. Complete details and results of the testing program are presented by Cho (2007).

Burland (1989) suggested that working strain levels in soil around well-designed tunnels and foundations were on the order of 0.1 %. If one uses data collected with conventional triaxial equipments to discern the soil responses, one can reliably measure strains 0.1% or higher. Thus in many practical situations, it is not possible to accurately incorporate site-specific small strain non-linearity into a constitutive model based on conventionally-derived laboratory data.

Model selection

There are a number of models reported in literature wherein the variation of small strain nonlinearity can be represented, for example, a three-surface kinematic model develop for stiff London clay (Stallebrass and Taylor 1997), MIT-E3 (Whittle and Kavvadas 1994), hypoplasticity models (e.g. Viggiani and Tamagnini 1999), and a directional stiffness model (Tu 2007). These models require either detailed experimental results or experience with the model in a given geology to derive parameters. While the models can be implemented in material libraries in some commercial finite element codes, these routines are not readily available to most practitioners. Thus for most current practical applications, one uses simpler, elasto-plastic models contained in material libraries in commercial codes.

For these models, a key decision is to select the elastic parameters that are representative of the secant values that correspond to the predominant strain levels in the soil mass. Examples of the strain levels behind a wall for an excavation with lateral wall movements of 29 and 57 mm are shown in Figure 5. These strain levels were computed based on the results of displacement-controlled simulations where the lateral wall movements and surface settlements were incrementally applied to the boundaries of a finite element mesh. The patterns of movements were typical of excavations through clays, and were based on those observed at an excavation made through Chicago clays (Finno and Blackburn 2005). Because the simulations were displacement-controlled, the computed strains do not depend on the assumed constitutive behavior.

As can be seen in Figure 5, the maximum shear strains correspond to about 0.3% for 29 mm maximum wall lateral movement, and represent good control of ground movements in these soft soils. Shear strains as high as 0.7% occurred when 57 mm of maximum wall movement develop. These strain levels can be accurately measured in conventional triaxial testing, and thus if one can obtain specimens of sufficiently high quality, then secant moduli corresponding to these strain levels can be determined via
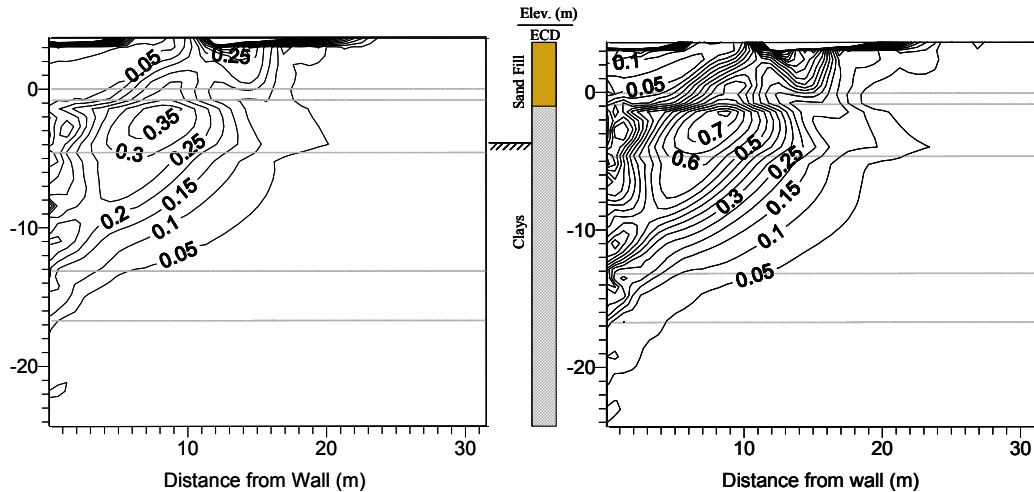
(a) 29 mm maximum wall movement   **(b)** 57 mm maximum wall movement

Fig. 5. Shear strain levels behind excavation (contours in %)

conventional laboratory testing. Because the maximum horizontal wall displacement can be thought of as a summation of the horizontal strains behind a wall, the maximum wall movements can be accurately calculated with a selection of elastic parameters that corresponds to these expected strain levels. In this case, the fact that small strain non-linearity is not explicitly considered will not have a large impact on the computed horizontal wall displacements because they are dominated by the larger strains in the soil mass. Consequently, these computed movements would be compatible with those measured by an inclinometer located close to the wall.

However, if one needs to have an accurate representation of the distribution of ground movements with distance from the wall, then this approach of selecting strain-level appropriate elastic parameters will not work. The small strain non-linearity must be explicitly considered to find the extent of the settlement because the strains in the area of interest vary from the maximum value to zero. As a consequence, many cases reported in literature indicate computed wall movements agree reasonably well with observed values, but the results from the same computations do not accurately reflect the distribution of settlements. Good agreement at distances away from a wall can be obtained only if the small stain non-linearity of the soil is adequately represented in the constitutive model.

The relation between lateral wall displacements and shear strain levels in the soil behind the wall can be evaluated from results of displacement-controlled finite element simulations. Similar to the results shown in Figure 5, different displacement profiles were studied by imposing lateral wall displacements and settlement profiles, representing conditions with maximum lateral movements at the excavated surface, cantilever movements, deep-seated movements and combination of the last two. The stratigraphies used in the models were based on typical Chicago soils. The results in Figure 6 show that the relationship between maximum shear strain behind the wall and maximum displacement of the wall is almost linear for lateral wall displacements between 10 and 110 mm. Figure 6 also shows that the results form a narrow band,

suggesting that the relation between strain and wall displacement is not greatly affected by the type of movement.

Figure 6 can be used to estimate shear strains for a specified maximum wall movement. With this value of shear strain, the secant shear moduli for use in conventional elasto-plastic models can be estimated based on strain-stress data from high quality lab tests. The values of maximum shear strains, even in the cases with the relatively low values of displacements, are about 0.2% and increase as the specified displacement becomes larger. This is important when one determines soil stiffness in the lab. Conventional soil testing without internal instrumentation allows one to accurately measure strains as low as 0.1%. Thus for many cases, the secant shear moduli can be determined from conventional laboratory tests. However, if strain levels are 0.2% or less, then one must select these moduli from test results based on internally-measured strains in equipment not normally available in commercial laboratories.
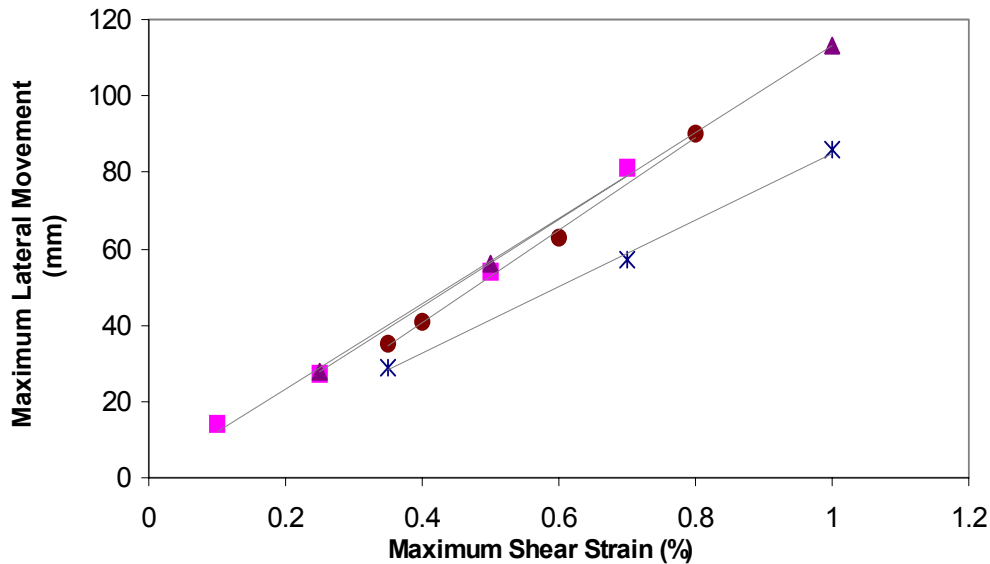
Fig. 6. Relation between maximum wall movement and shear strain

In summary, using a simulation based on conventional elasto-plastic models limits the type and location of the data that can be used as observations in an inverse analysis. Both vertical and lateral movements measured at some distance from a wall cannot be calculated accurately in this case because the variation of stiffness with strain levels must be adequately represented in the soil model. Only the lateral movements close to a support wall can be reasonably computed with conventional models since that result is dominated by the zones of high strains behind the wall.

MONITORING DATA

The assumptions inherent in any prediction limit the types of data that can be used as a basis of updating performance predictions. Consequently, one must carefully select the types of data, location of the measuring points, and the excavation conditions

when applying an inverse technique. Inclinometer data based on measurements close to a support wall are the most useful when typical elasto-plastic constitutive models are assumed to represent soil behavior, as is the case when employing commercial finite element codes, for reasons discussed in the last section. These data can be supplemented by ground surface settlements when using a constitutive model that accounts for small strain nonlinearities and dilation (Finno and Tu 2006). Furthermore, other types of measurements, such as forces in internal braces and pore water pressures, conceptually can be used in conjunction with displacement measurements to make the computed results more sensitive to parameters selected for optimization (Rechea 2006).

While these different types of data can be handled within a properly formulated inverse analysis, the timely collection and screening of the data currently presents an obstacle to use this approach in current practice. However, many papers at this conference discuss advances that eventually will make possible fully automated systems that can continuously monitor ground and structural responses due to excavation activities and provide an engineer with an uninterrupted stream of data in near real time. These systems are essential tools for making timely decisions regarding construction activities to mitigate potential damage to adjacent facilities.

Briefly, remotely sensed total survey stations can be established to monitor the displacement of optical prisms (e.g. Finno and Blackburn 2005). In-place inclinometers can be deployed to remotely measure lateral movements of the walls of the support system and the adjacent ground. Vibrating wire piezometers can be installed to monitor pore water pressures in the adjacent ground. Strain gauges can be mounted on structural supports to measure strains at discrete points in internal braces of temporary support systems (e.g. Finno et al. 2005) due to earth loading, self-weight, temperature changes, and unexpected construction loading. A Brillouin optical time-domain reflectometer, recently developed by Nippon Telegraph and Telecommunications Corp., can be deployed to measure strains along an optical fiber and provide a complete strain profile (Vorster et al. 2006). Tiltmeters can be mounted on structural elements and results used to compute the angular distortion of an affected structure.

To correlate the numerical data with the causative actions of the excavation process, imaging technologies can be employed to provide an accurate and detailed record of construction activities. Three-dimensional laser scanning is a relatively new technology that utilizes LIDAR (Light Detection and Ranging). Trupp et al. (2004) used 3-D laser scanning to capture an accurate image of the geometry of the excavation to provide an accurate, as-built digital record of construction. Sections may be taken from these scans and imported into a finite element code to provide an accurate excavation surface for input to inverse analysis. An internet accessible weather-resistant video camera has been used on several projects to allow remote visualization of the construction process in real-time, as well as a dated, photographic record of construction (Finno and Blackburn 2005).

INVERSE ANALYSIS

In model calibration, various parts of the model are changed so that the measured values are matched by equivalent computed values until the resulting calibrated

model accurately represents the main aspects of the actual system. In practice, numerical models typically are calibrated using trial-and-error methods. Inverse analysis works in the same way as a non-automated calibration approach: parameter values and other aspects of the model are adjusted until the model's computed results match the observed behavior of the system.

Inverse analysis techniques have been applied to geotechnical problems since the 1980s (e.g., Gioda and Maier 1980; Sakurai and Takeuchi 1983). Its use allows one to evaluate performance of geotechnical structures by a quantifiable observational method. It has been used to identify soil parameters from laboratory or in situ tests (e.g., Anandarajah and Agarwal 1991), and performance data from excavation support systems (e.g., Ou and Tang1994; Calvello and Finno 2004; Finno and Calvello 2005; Levasseur et al. 2007), excavation of tunnels in rock (Sakurai and Takeuchi, 1983; Gens et al. 1996) and embankment construction on soft soils (Arai et al., 1986; Wakita and Matsuo, 1994). Many of the previous evaluations of performance data were conducted with very simple soil models that severely restricted the ability of the computations to accurately reflect the observed field performance data, irrespective of employing inverse techniques.

Use of an inverse model provides results and statistics that offer numerous advantages in model analysis and, in many instances, expedites the process of adjusting parameter values. The fundamental benefit of inverse modeling is its ability to calculate automatically parameter values that produce the best fit between observed and computed results. The main difficulties inherent to inverse modeling algorithms are complexity, non-uniqueness, and instability. Complexity of real, non-linear systems sometimes leads to problems of insensitivity when the observations do not contain enough information to support estimation of the parameters. Non-uniqueness may result when different combinations of parameter values match the observations equally well. Instability can occur when slight changes in model variables radically change inverse model results. Although these potential difficulties make inverse models imperfect tools, work in related civil engineering fields (e.g., Poeter and Hill, 1997) demonstrate that inverse modeling provides capabilities that help modelers significantly, even when the simulated systems are very complex.

Two main types of inverse analysis have been applied to geotechnics, optimization by iterative algorithms such as gradient methods (e.g., Ou and Tang 1994; Ledesma et al., 1996; Calvello and Finno 2004) and optimization by techniques from the field of artificial intelligence, including artificial neural networks (Yamagami et al. 1997; Hashash et al. 2006) and genetic algorithms (Levasseur et al. 2007). These methods are distinguishable by their physical approach. The gradient method employs a local parameter identification of a specific constitutive law. The artificial neural network is a method which creates by learning phases its own constitutive law from geotechnical measurements. Genetic algorithms are global optimization methods which localize an optimum set of solutions close to the "true" value.

Gradient Method of Inverse Analysis

In the work described herein, model calibration by inverse analysis with a gradient method is conducted using UCODE (Poeter and Hill, 1998), a computer code designed to allow inverse modeling posed as a parameter estimation problem. Macros

can be written in a windows environment to couple UCODE with any application software.
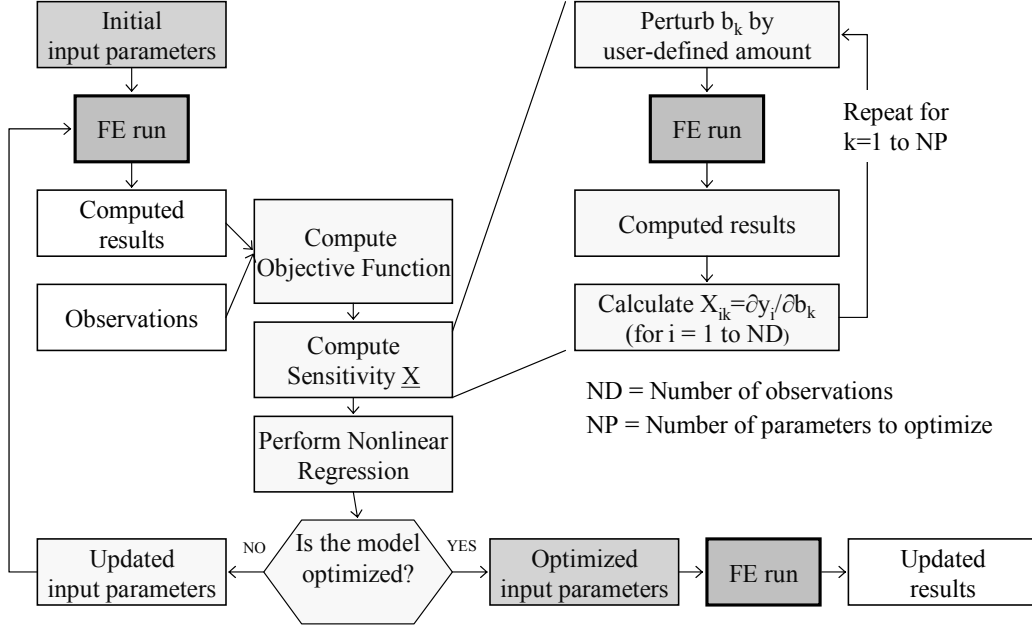
Fig. 7. Flow chart for inverse analysis

Figure 7 shows a flowchart of the parameter optimization algorithm used in UCODE. With the results of a finite element prediction in hand, the computed results are compared with field observations in terms of weighted least-squares objective function, S($\underline{b}$):

$$S\left(\underline{b}\right)=\left[\underline{y}-\underline{y}'\left(\underline{b}\right)\right]^{T}\underline{\omega}\left[\underline{y}-\underline{y}'\left(\underline{b}\right)\right]=\underline{e}^{T}\underline{\omega}\underline{e} \tag{5}$$

where $\underline{b}$ is a vector containing values of the parameters to be estimated; $\underline{y}$ is the vector of the observations being matched by the regression; $\underline{y}'(\underline{b})$ is the vector of the computed values which correspond to observations; $\underline{\omega}$ is the weight matrix wherein the weight of every observation is taken as the inverse of its error variance; and $\underline{e}$ is the vector of residuals. This function represents a quantitative measure of the accuracy of the predictions.

A sensitivity matrix, $\underline{X}$, is then computed using a forward difference approximation based on the changes in the computed solution due to slight perturbations of the estimated parameter values. This step requires multiple runs of the finite element code. Regression analysis of this non-linear problem is used to find the values of the parameters that result in a best fit between the computed and observed values. In UCODE, this fitting is accomplished with the modified Gauss-Newton method, the results of which allow the parameters to be updated using:

$$\left(\underline{C}^{T}\underline{X}^{T}{}_{r}\underline{\omega}\underline{X}_{r}\underline{C}+\underline{I}m_{r}\right)\underline{C}^{-1}\underline{d}_{r}=\underline{C}^{T}\underline{X}^{T}{}_{r}\underline{\omega}\left(\underline{y}-\underline{y}'\left(\underline{b}_{r}\right)\right) \tag{6}$$

$$\underline{b}_{r+1}=\rho_{r}\underline{d}_{r}+\underline{b}_{r} \tag{7}$$

where d_r is the vector used to update the parameter estimates b; r is the parameter estimation iteration number; X_r is the sensitivity matrix ($X_{ij}=\partial y_i/\partial b_j$) evaluated at parameter estimate $\underline{b}_r$; $\underline{C}$ is a diagonal scaling matrix with elements c_{jj} equal to $1/\sqrt{(\underline{X}^T\underline{\omega}\,\underline{X})_{jj}}$; $\underline{I}$ is the identity matrix; m_r is the Marquardt parameter used to improve regression performance; and ρ_r is a damping parameter, computed as the change in consecutive estimates of a parameter normalized by its initial value, but is restricted to values less than 0.5.

At a given iteration, after performing the modified Gauss-Newton optimization, the updated model is considered optimized if either of two convergence criteria is met:

  i. the maximum parameter change of a given iteration is less than a user-defined percentage of the value of the parameter at the previous iteration;
  ii. the objective function, S($\underline{b}$), changes less than a user-defined amount for three consecutive iterations.

After the model is optimized, the final set of input parameters is used to run the finite element model one last time and produce the "updated" prediction of future performance. See Rechea (2006) for details concerning the convergence criteria as applied to excavations.

Weighting Function

The weight of an observation can be expressed as the inverse of the variance for the 95% confidence interval for the accuracy of a measurement:

$$weight = \frac{1}{\sigma^2} \qquad \sigma = \frac{Accuracy}{1.96} \qquad (8)$$

In this way, more reliable data (smaller variability) are given greater emphasis, or weight. The errors associated to measurements are usually related to the accuracy of the instrumentation, and independent of the magnitude of the observation (assuming the observation is within the range of the instrumentation). Table 1 shows how to obtain weights for various types of instrumentation. Accuracies and ranges in Table 1 are taken from manufacturer's literature, and are meant to be representative of typical values in the field. Smaller values can be used based on field data collected prior to any activity at the site, assuming enough data are collected to adequately define the variation about the initial value (Langousis 2007).

Selection of Parameters

The relative importance of the input parameters being simultaneously estimated can be defined using various parameter statistics (Hill 1998). The statistics found useful for this type of work are the composite scaled sensitivity, ccs_j, and the correlation coefficient, $cor(i,j)$. The value of css_j indicates the total amount of information provided by the observations for the estimation of parameter j, and is defined as:

$$css_j = \left[\sum_{j=1}^{ND} \left(\left(\frac{\partial y'_i}{\partial b_j} \right) b_j \omega_{ii}^{1/2} \right)^2 \Bigg|_{\underline{b}} \Bigg/ ND \right]^{1/2} \tag{9}$$

where y'_i is the ith computed value, b_j is the jth estimated parameter, $\partial y_i/\partial b_j$ is the sensitivity of the ith computed value with respect to the jth parameter, ω_{jj} is the weight of the ith observation, and ND is the number of observations.

Table 1. Typical weights of observations

Instrumentation	Range (full scale)	Accuracy	95% standard deviation, σ	Weight
Lateral movements with inclinometers	$\pm 53°$ from vertical	± 0.25 mm/m $\dfrac{0.25}{1000} \cdot d$	$\dfrac{0.25}{1000} \cdot \dfrac{d}{1.96} = 0.0001 \cdot d$ (m)	$\dfrac{1}{(0.0001 \cdot d)^2}$
		where d is distance (m) from bottom of casing		
Ground surface settlement with optical survey		± 0.01 ft ± 0.003 m	$\dfrac{0.003}{1.96} = 0.00155$ (m)	$\dfrac{1}{(0.00155)^2}$
vibrating wire piezometer	3.5 bar/50 psi 344.8 Pa	$\pm 0.1\%$ FS ± 0.34 Pa	$\dfrac{0.34}{1.96} = 0.173$ (Pa)	$\dfrac{1}{(0.173)^2}$
Strut force with spot-weldable strain gauge	2,500 microstrain	$\pm 0.1\%$FS $= \pm 2.5$ microstrain	$\dfrac{E \cdot A \cdot Accuracy}{1.96}$ (kN)	$\dfrac{1}{(6.19)^2}$ (1)

[1] value shown is for a steel brace with A = 0.024 m^2

The values of the matrix *cor (i,j)* indicate the correlation between the ith and j^{th} parameters, and are defined as:

$$cor(i, j) = \frac{\text{cov}(i, j)}{\text{var}(i)^{1/2} \, \text{var}(j)^{1/2}} \tag{10}$$

where cov(i,j) equal the off-diagonal elements of the variance-covariance matrix $\underline{V}(\underline{b}') = s^2(\underline{X}^T\omega\underline{X})^{-1}$, and var($i$) and var($j$) refer to the diagonal elements of $\underline{V}(\underline{b}')$.

Inverse analysis algorithms allow the simultaneous calibration of multiple input parameters. However, identifying the important parameters to include in the inverse analysis can be problematic, and it is not possible to use a regression analysis to estimate every input parameter of a given excavation simulation. The number and type of input parameters that one can expect to estimate simultaneously depend on a number of factors, including the soil models used, the stress conditions of the simulated system, available observations, and numerical implementation issues.

Figure 8 shows a procedural flowchart that can be used for the identification of the soil parameters to optimize by inverse analysis. The total number of input parameters can be reduced, in three steps, to the number of parameters that are likely to be optimized successfully by inverse analysis.
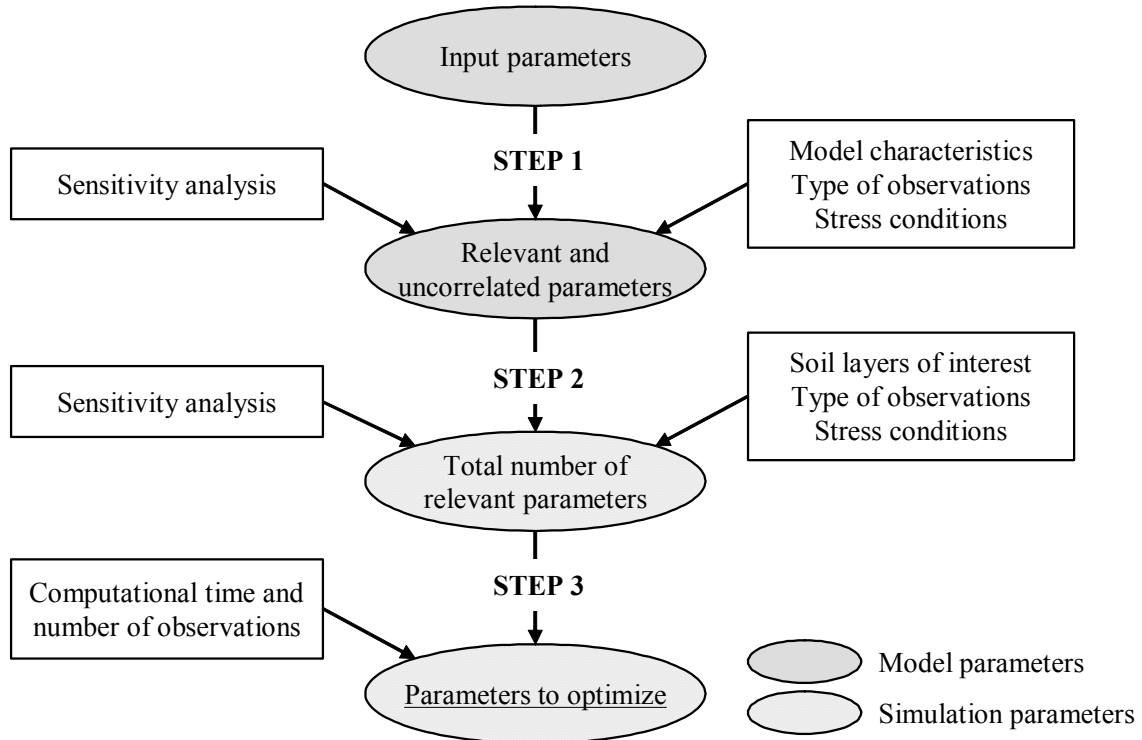
Fig. 8. Identification of soil parameters to optimize by inverse analysis (Finno and Calvello 2005)

In step 1 the number of relevant and uncorrelated parameters of the constitutive model chosen to simulate the soil behavior is determined. The number of parameters that can be estimated by inverse analysis depends upon the characteristics of the model, the type of observations available, and the stress conditions in the soil. Composite scaled sensitivity values (Eq. 9) can provide valuable information on the relative importance of the different input parameters of a given model. Parameter correlation coefficients (Eq. 10) can be used to evaluate which parameters are correlated and are, therefore, not likely to be estimated simultaneously by inverse analysis. In step 2 the number of soil layers to calibrate and the type of soil model used to simulate the layers determines the total number of relevant parameters of the simulation. An additional sensitivity analysis may be necessary to check for correlations between parameters relative to different layers. Finally, in step 3, the total number of observations available and computational time considerations may prompt a final reduction of the number of parameters to optimize simultaneously. An example of this procedure is presented by Calvello and Finno (2004).

EXAMPLES OF INVERSE ANALYSIS

Several examples of inverse analyses applied to supported excavations are presented to illustrate (i) its ability to identify optimized parameters based on observations made during early stages of excavation so as to allow accurate predictions of performance of latter stages of an excavation, and, (ii) the applicability of optimized parameters found based on performance data of one excavation to others in the same geology.

The finite element software PLAXIS was used to compute the plane strain response of the soil around these excavations. The inverse techniques contained in UCODE can be coupled with any application software, and it also has been successfully coupled with ABAQUS and other research-oriented finite element codes. For purposes of brevity, only PLAXIS applications with the hardening-soil model (H-S) (Schanz et al. 1999) are presented in this paper. Parameters from other constitutive models have been optimized as well (e.g., Calvello and Finno 2002).

The effective stress H-S model is formulated within the framework of elasto-plasticity. Plastic strains are calculated assuming multi-surface yield criteria. Isotropic hardening is assumed for both shear and volumetric strains. The flow rule is non-associative for frictional shear hardening and associative for the volumetric cap. Six basic H-S input parameters define the constitutive soil responses, the friction angle, φ, cohesion, c, dilation angle, ψ, the reference secant Young's modulus at the 50% stress level, E_{50}^{ref}, the reference oedometer tangent modulus, E_{oed}^{ref}, and the exponent m which relates reference moduli to the stress level dependent moduli (E representing E_{50}, E_{oed}, and E_{ur}):

$$E = E^{ref}\left(\frac{c \cot \phi - \sigma_3^{'}}{c \cot \phi + p^{ref}} \right)^m \tag{11}$$

where p^{ref} is a reference pressure equal to 100 stress units and σ'_3 is the minor principal effective stress. A sensitivity analysis indicated that the model's relevant and uncorrelated parameters for the Chicago excavations presented herein are E_{50}^{ref} and ϕ (Calvello and Finno 2004). Results were also sensitive to changes in values of parameter m. However, parameter m was not included in the regression because the values of the correlation coefficients between parameters m and E_{50}^{ref} were very close to 1.0 at every layer, indicating that the two parameters were not likely to be simultaneously and uniquely optimized. When values of ϕ were kept constant at their initial estimates, and only the stiffness parameters, E_{50}^{ref}, were optimized, the calibration of the simulations presented subsequently was successful. Finno and Calvello (2005) showed that shear stress levels in the soil around the excavation were much less than those corresponding to failure for the great majority of the soil. This is indeed expected for excavation support systems that are designed to restrict adjacent ground movements to acceptably small levels, and hence one would expect the stiffness parameters to have a greater effect on the simulated results than failure parameters.

Parameter Optimization at Early Stages of Excavation

The ability of the approach to provide optimized parameters at an early stage of excavation which leads to good predictions of subsequent performance is illustrated by the Chicago Ave. and State St. subway renovation project in Chicago (Finno et al. 2002). This project involved the excavation of 12.2 m of soft to medium clay within 2 m of a school supported on shallow foundations. Figure 9 shows a section of the excavation support system. The support system consisted of a secant pile wall with three levels of support, which included pipe struts (1st level) and tieback anchors (2nd and 3rd levels).
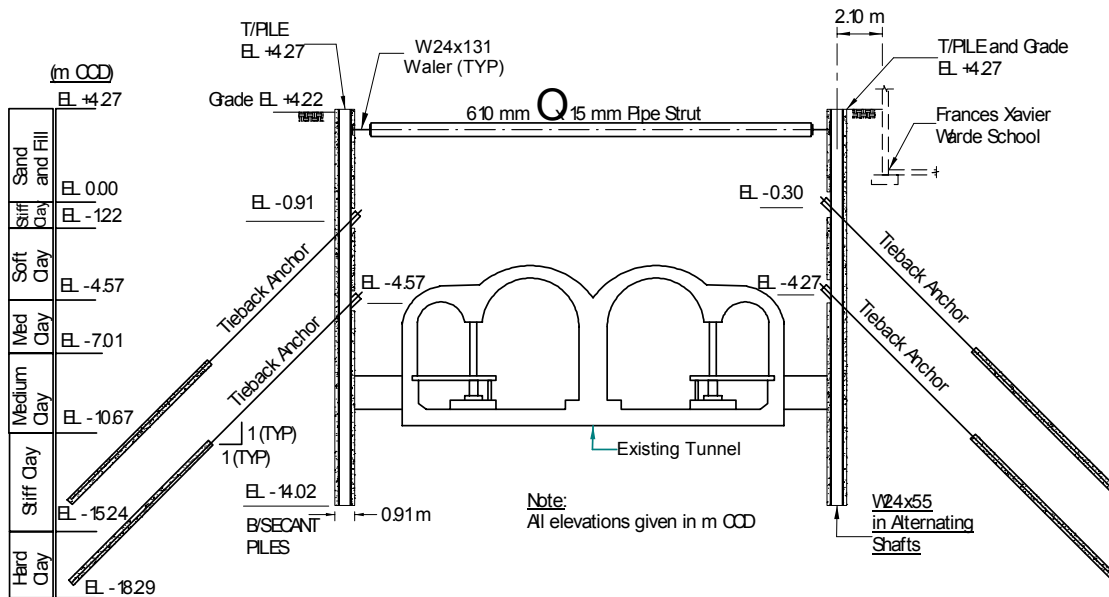
Fig. 9. Support system for Chicago-State excavation (Finno et al. 2002)

The subsurface conditions consisted of an urban fill, mostly medium dense sand but also containing construction debris, overlying four strata associated with the repetitive process of advance and retreat of the Wisconsin glacier. The upper three are ice margin deposits deposited underwater, and are distinguished by water content and undrained shear strength (Chung and Finno, 1992). With the exception of a clay crust in the upper layer, these deposits are lightly overconsolidated as a result of lowered groundwater levels after deposition and/or aging. Stratigraphy is shown in terms of Chicago City Datum (CCD) elevation.

A complete record of performance of the excavation can be found in Finno et al. (2005). Figure 10 summarizes deformation responses to excavation and support. Both lateral movements and settlements are shown. The movements that occurred as the secant pile wall extend through all compressible layers. This is important when using these observations to calibrate parameters using inverse techniques in that these

movements occur at an early stage of the excavation, and hence contain information that can be used to optimize parameters in all layers that can be useful to predict movements at subsequent stages of excavation.
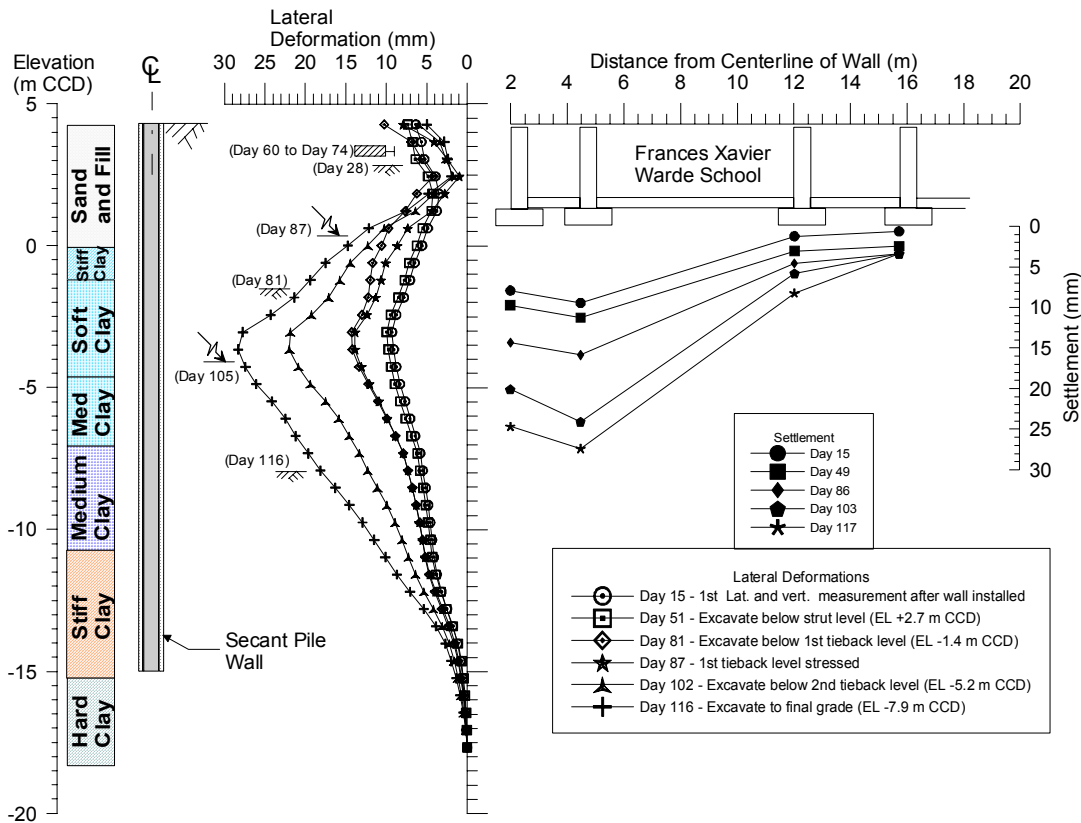
Fig. 10. **Lateral movements and settlements at Chicago-State excavation (Finno et al. 2002)**

Very little movement beyond that which occurred during wall installation were observed until the excavation was lowered below elev. −1.4 m CCD; a maximum of 4 mm additional lateral movement occurred as a result of excavating to this elevation. This behavior suggests that the upper clays initially are relatively stiff, and provide field indications of the small strain nonlinearity of these soils. After wall installation, the secant pile wall incrementally moved toward the excavation in response to excavation-induced stress relief. When the excavation reached final grade, the maximum lateral movement was 28 mm. The school settled as the secant pile wall moved laterally. The maximum settlement at the school at the end of excavation was also 28 mm.

Table 2 shows the calculation phases and the construction stages used in the finite element simulations. Note that the tunnel tubes and the school adjacent to the excavation were explicitly modeled in the first 12 phases of the simulation to take into account the effect of their construction on the soil surrounding the excavation. Stages 1, 2, 3, 4 and 5 in the optimization process refer to the construction stages for which the computed results were compared to inclinometer data taken from two

inclinometers on opposite sides of the excavation. Construction steps not noted as "consolidation" on Table 2 were modeled as undrained. Consolidation stages were included after the tunnel, school and wall installation calculation phases to permit excess pore water pressures to equilibrate. To simulate secant pile wall installation in the plane strain analysis, elements representing the wall were excavated and a hydrostatic pressure equivalent to a water level located at the ground surface was applied to the face of the resulting trench (calculation phase 13 in Table 2). After computing the movements associated with this process, the excavated elements were replaced by elements with the properties of the secant pile wall (calculation phase 14). Details about the definition of the finite element problem, the calculation phases and the model parameters used in the simulation can be found in Calvello (2002).

Table 2. FE simulation of construction.

Phase	Construction step	Simulation stage
0	Initial conditions	
1-4	Tunnel construction (1940)	
5	Consolidation	
6-10	School construction (1960)	
11-12	Consolidation	
13	Drill secant pile wall (1999)	
14	Place concrete in wall	**Stage 1**
15	Consolidation (20 days)	
16	Excavate and install struts	**Stage 2**
17	Excavate below first tieback level	
18	Prestress first level of tiebacks	**Stage 3**
19	Excavate below second tieback level	
20	Prestress second level of tiebacks	**Stage 4**
21	Excavate to final grade	**Stage 5**

Visual examination of the horizontal displacement distributions at the inclinometer locations provides the simplest way to evaluate the fit between computed and measured field response. When computations were made based on parameters derived from results of drained triaxial tests, the finite element model computed significantly larger displacements at every construction stage (Finno and Calvello 2005). The maximum computed horizontal displacements are about two times the measured ones and the computed displacement profiles result in significant and unrealistic movements in the lower clay layers. As one would expect, these results indicated that the stiffness properties for the clay layers based on conventional laboratory data were less than field values.

Figure 11 shows the comparison between the measured field data from both sides of the excavation and the computed horizontal displacements when parameters are optimized based on stage 1 observations. The improvement of the fit between the computed and measured response is significant. Despite the fact that the optimized set of parameters is calculated using only stage 1 observations, the positive influence on the calculated response is substantial for all construction stages. At the end of the construction (i.e. stage 5) the maximum computed displacement exceeds the

measured data by only about 15%. These results are significant in that a successful recalibration of the model at an early construction stage positively affects subsequent "predictions" of the soil behavior throughout construction.
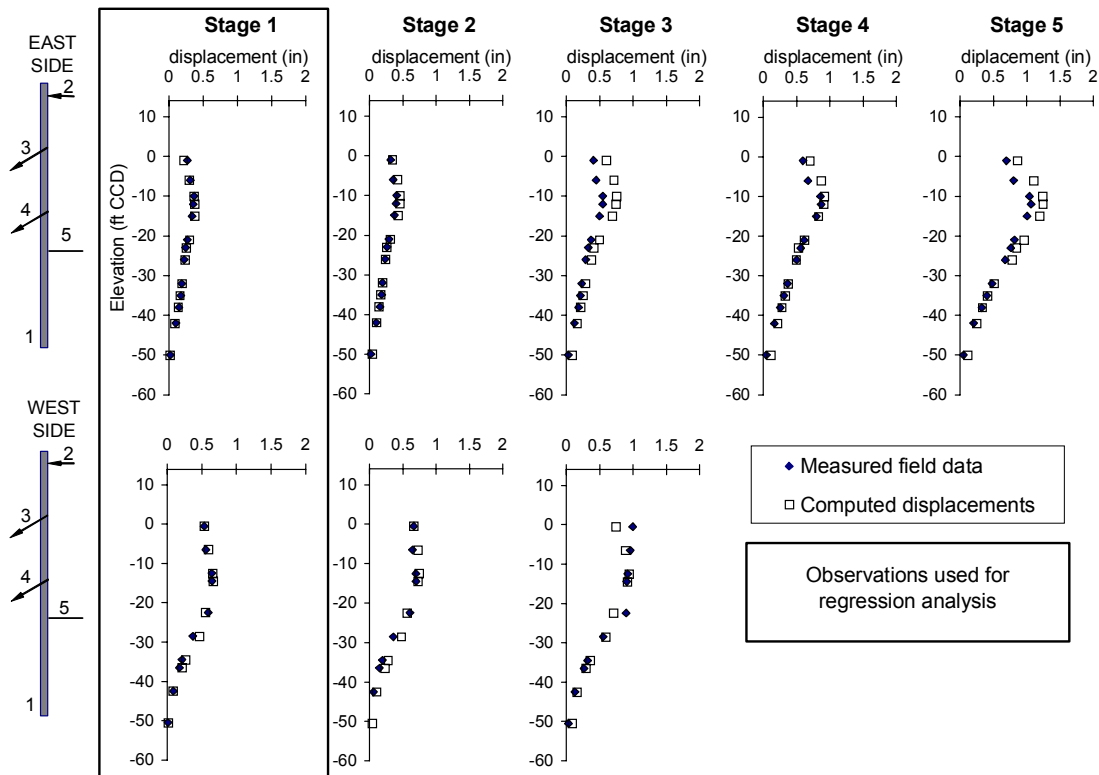
Fig. 11. Comparison of observed and computed horizontal displacements (after Finno and Calvello 2005)

Analyses were also made wherein parameters were recalibrated at every stage until the final construction stage (stage 5). At every new construction stage, the inclinometer data relative to that stage were added to the observations already available. Results indicated that difference between the fit shown in Figure 6 and with those calibrated after every increment was not significant. In essence, the inverse analysis performed after the first construction stage "recalibrated" the model parameters in such a way that the main behavior of the soil layers could be accurately predicted throughout construction.

Applicability of Optimized Parameters at Other Locations in Same Deposit

To show the applicability of the optimized parameters that formed the basis of the good agreement in Figure 11 to other excavation sites in these soil deposits, the results of numerical simulations are presented in Figure 12 based on these optimized parameters for the Lurie (Finno and Roboski 2005) and the Ford Design Center (Blackburn and Finno 2007) excavations. The geologic origin of the most compressible material is similar for all three cases, but the Lurie Center is located

about 2 km from the Chicago-State site and the Ford Center is located about 15 km from the site. Consequently one should expect some variability in the actual parameters at each site.
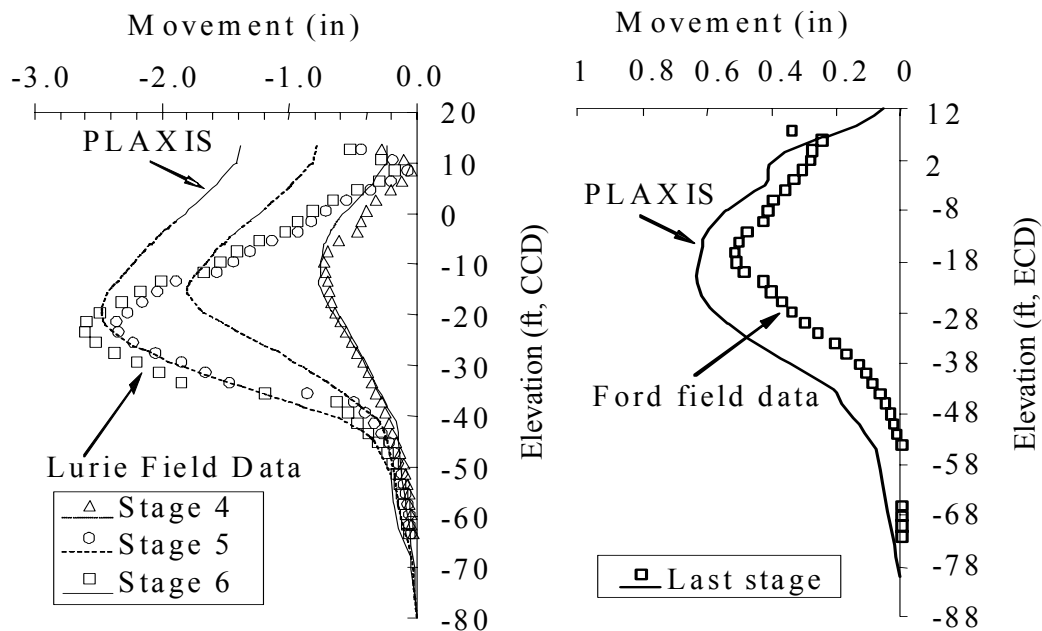
Figure 12. Computed and observed lateral movements based on optimized parameters from Chicago-State excavation

Examining the comparisons in the clay layers below – 15 ft CCD for the Lurie data, reasonable agreement is observed at stages 4 and 6, with significant differences seen at the intermediate stage 5. While the reasons for this are not entirely clear, the difference between the excavated levels for stages 5 and 6 was only 2 m. The observed lateral movements from stage 5 might have been impacted by the excavation process not being completely uniform. This emphasizes the need to carefully select stages for analysis that are compatible with the assumed numerical model – in this case a plane strain representation of the problem. While care was taken to do so, some simplification of the excavation process was necessary in order to obtain a complete record of the responses. Furthermore, the computed results indicated much larger cantilever type movements than were observed. As mentioned before, this difference was due to the representation of the tiebacks in the plane strain simulation.

At the Ford Center, the numerical results shown in Figure 12 followed similar trends as the observed data, but with larger magnitudes. This is likely caused by the fact that the H-S model used herein does not include provisions to represent the large stiffness degradation with small strains. One must select moduli that represent the average strains within the soil mass, and when the movements are small, the average modulus should be higher in a model that does not consider the small strain modulus degradation. The parameters used in the analysis were based on the larger

deformations that were present at the Chicago-State site, and hence resulted in larger deformations than were observed at the Ford Center. In any case, the application of the Chicago-State based optimized parameters to both the Lurie and Ford sites resulted in reasonable agreement with the observed lateral movements, within the limitations of the analyses. Application of the inverse techniques to these data resulted in improved fit with minor changes to the parameters (Rechea 2006).

CONCLUDING REMARKS

This paper discusses use of monitoring data to update performance predictions of supported excavations. Successful applications of this approach depend equally on reasonable numerical simulations of performance, the type of monitoring data used as observations, and the inverse analysis techniques used to minimize the difference between predictions and observed performance.

The calibration by inverse analysis of the various simulations presented herein indicated that the numerical methodology developed to optimize a finite element model of an excavation can be very effective in minimizing the errors between the measured and computed results. However, the convergence of an inverse analysis to an "optimal solution" (i.e. best-fit between computed results and observations) does not necessarily mean that the simulation is satisfactorily calibrated. A geotechnical evaluation of the optimized parameters is always necessary to verify the reliability of the solution. For a model to be considered "reliably" calibrated both the fit between computed and observed results must be satisfactory (i.e. errors are within desired and/or accepted accuracy) and the best-fit values of the model parameters must be reasonable.

The key to the successful calibration of an excavation lies in defining a "well posed" inverse analysis problem to calibrate the simulation. The parameters optimized by inverse analysis are few compared to the total number of parameters defining the behavior of the simulation. Indeed, the majority of the input parameters is estimated by conventional means and never "re-calibrated." Yet, the optimization can be extremely effective if a finite element simulation of the excavation adequately reproduces the stress history of the soil on site and the soil model adequately represented the behavior of the clays, at least in terms of appropriate field observations. In the cases presented herein with ground responses modeled by a conventional elasto-plastic soil model, the constitutive parameters that were relevant to the problem under study were calibrated based on inclinometer data obtained close to the support walls.

ACKNOWLEDGEMENTS

REFERENCES

Anandarajah A. and Agarwal D. (1991). "Computer-aided calibration of soil plasticity model." *International Journal for Numerical and Analytical Methods in Geomechanics* Vol. 15, 835-856.

Arai K., Ohta H. and Kojima K. (1986). "Application of back analysis to several test embankments on soft clay deposits." *Soils and Foundations*. Vol.26(2), 60-72.

Burland, J.B. (1989). "'Small is beautiful' – the stiffness of soils at small strains: Ninth Laurits Bjerrum Memorial Lecture." *Canadian Geotechnical Journal*, Vol. 26, 499-516.

Carter , J.P., Booker, J.R. and Small, J.C. (1979). "The analysis of finite elasto-plastic consolidation." *International Journal for Numerical and Analytical Methods in Geomechanics*, Vol. 3, 107-129.

Calisto, L. and Calebresi, G. (1998). "Mechanical behavior of a natural soft clay." *Geotechnique*, Vol. 48 (4), 495-513.

Calvello, M. (2002). "Inverse Analysis of a Supported Excavation through Chicago Glacial Clays," PhD thesis, Northwestern University, Evanston, IL.

Calvello M. and Finno R.J. (2002). "Calibration of soil models by inverse analysis." *Proc. International Symposium on Numerical Models in Geomechanics, NUMOG VIII*, Balkema, p. 107-116.

Calvello M. and Finno R.J. (2003). "Modeling excavations in urban areas: effects of past activities." *Italian Geotechnical Journal*, 37(4), 9-23.

Calvello M. and Finno R.J. (2004). "Selecting parameters to optimize in model calibration by inverse analysis." *Computers and Geotechnics*, Elsevier, Vol. 31, 5, 2004, 411-425.

Chung, C.-K. and Finno, R.J. (1992). "Influence of Depositional Processes on the Geotechnical Parameters of Chicago Glacial Clays," *Engineering Geology*, 32, 225-242.

Christian, J. T. and Wong, I.H. (1973). "Errors in simulation of excavation in elastic media by finite elements." *Soils and Foundations*, Vol. 13 (1), 1-10.

Cho, W.J. (2007). "Recent stress history effects on compressible Chicago glacial clay," PhD thesis, Northwestern University, Evanston, IL.

Clayton, C.R.I., and Heymann, G. (2001). "Stiffness of geomaterials at very small strains." *Geotechnique*, Vol. 51 (3), 245-255.

Clough, G.W. and Mana, A. I. (1976). "Lessons learned in finite element analysis of temporary excavations." *Proceedings, 2nd International Conference on Numerical Methods in Geomechanics*, ASCE, Vol. I, 496-510.

Clough, G.W. and Tsui, Y. (1974). "Performance of tied-back walls in clay." *Journal of the Geotechnical Engineering Division*, ASCE, Vol. 100 (12), 1259-1274.

Clough, G. W., Smith, E.M., and Sweeney, B.P. (1989). "Movement control of excavation support systems by iterative design." *Current Principles and Practices, Foundation Engineering Congress,* Vol. 2, ASCE, 869-884.

Finno, R.J., Atmatzidis, D.K., and Nerby, S.M. (1988). "Ground response to sheet-pile installation in clay," *Proceedings, Second International Conference on Case Histories in Geotechnical Engineering*, St. Louis, MO.

Finno, R.J., Atmatzidis, D.K., and Perkins, S.B. (1989). "Observed Performance of a Deep Excavation in Clay," *Journal of Geotechnical Engineering*, ASCE, Vol. 115 (8), 1045-1064.

Finno, R.J. and Blackburn, J.T. (2005). "Automated monitoring of supported excavations," *Proceedings, 13th Great Lakes Geotechnical and Geoenvironmental Conference, Geotechnical Applications for Transportation Infrastructure,* GPP 3, ASCE, Milwaukee, WI., 1-12.

Finno R.J., Bryson L.S. and Calvello M. (2002). "Performance of a stiff support system in soft clay." *Journal of Geotechnical and Geoenvironmental Engineering*, ASCE, Vol. 128, No. 8, p. 660-671.

Finno, R.J. and Calvello, M. (2005). "Supported excavations: the observational method and inverse modeling." *Journal of Geotechnical and Geoenvironmental Engineering*. ASCE, 131 (7).

Finno, R.J., and Nerby, S.M., (1989). "Saturated Clay Response During Braced Cut Construction," *Journal of Geotechnical Engineering*, ASCE, Vol. 115, No. 8, 1065-1085.

Finno, R.J. and Roboski, J.F., (2005). "Three-dimensional Responses of a Tied-back Excavation through Clay," Journal of Geotechnical and Geoenvironmental Engineering, ASCE, Vol. 131, No. 3, 273-282.

Finno, R.J. and Tu, X. (2006). "Selected Topics in Numerical Simulation of Supported Excavations," *Numerical Modeling of Construction Processes in Geotechnical Engineering for Urban Environment,* International Conference of Construction Processes in Geotechnical Engineering for Urban Environment, Th. Triantafyllidis, ed., Bochum, Germany, Taylor & Francis, London, 3-20.

Ghaboussi, J. and Pecknold, D.A. (1985). "Incremental finite element analysis of geometrically altered structures." *International Journal of Numerical Methods in Engineering*. Vol 20(11) 2061-2064.

Gens A., Ledesma A., Alonso E.E. 1996. "Estimation of parameters in geotechnical backanalysis. - 2. Application to a tunnel excavation problem." *Computer and Geotechnics*. Vol. 18(1) pp.29-46.

Gourvenec, S.M. and Powrie, W. (1999). "Three-dimensional finite element analysis of diaphragm wall installation." *Geotechnique*, Vol. 49(6), 801-823.

Hashash, Y.M.A. and Finno, R.J. (2005). "Development of new integrated tools for predicting, monitoring and controlling ground movements due to excavations," *Proceedings, Underground Construction in Urban Environments*, ASCE Metropolitan Section Geotechnical Group, New York, NY,

Hashash Y.M.A., Marulanda C., Ghaboussi J. , Jung, S. (2006). "Novel approach to integration of numerical modeling and field observation for deep excavation." *Journal of Geotechnical and Geoenvironmental Engineering*, Vol. 132(8), pp.1019-1031.

Hill, M. (1998). "Methods and guidelines for effective model calibration." *U.S. Geological Survey. Water-resources investigations report 98-4005*.

Holman, T.P. (2005). "Small strain behavior of compressible Chicago glacial clay." PhD thesis, Northwestern University, Evanston, IL.

Hughes, T.J.R. (1980). "Generalization of selective integration procedures to anisotropic and nonlinear media." International *Journal of Numerical Methods in Engineering,* Vol. 15 (9), 1413-1418.

Jardine, R.J., Symes, M.J. and Burland, J.B. (1984). "The measurement of small strain stiffness in the triaxial apparatus." *Geotechnique*, Vol. 34 (3), 323-340.

Langousis, M.. (2007). "Automated Monitoring and Inverse Analysis of a Deep Excavation in Seattle," MS thesis, Northwestern University, Evanston, IL.

Levasseur S., Malécot Y., Boulon M., Flavigny E., (2007). "Soil parameter identification using a genetic algorithm." *International Journal for Numerical and Analytical Methods in Geomechanics*, in press.

Lings, M.L., Ng, C.W.W. and Nash, D.F.T. (1994). "The lateral pressure of wet concrete in diaphragm wall panels cast under bentonite." *Geotechnical Engineering,* Proceedings of the Institution of Civil Engineers, , 107, 163-172.

Mana, A.I. and Cough, G.W. (1981). "Prediction of movements for braced cut in clay." *Journal of Geotechnical Engineering*, ASCE, New York, Vol. 107, No. 8, 759-777.

O'Rourke, T.D. and Clough, G.W. (1990). "Construction induced movements of insitu walls." *Proceedings, Design and Performance of Earth Retaining Structures,* Lambe, P.C. and Hansen L.A. (eds). ASCE, 439-470.

O'Rourke, T.D. and O'Donnell, C.J. (1997). "Deep rotational stability of tiedback excavations in clay," *Journal of Geotechnical Engineering*, ASCE, Vol. 123(6), 506-515.

Ou, C.Y., Chiou, D.C. and Wu, T.S. (1996). "Three-dimensional finite element analysis of deep excavations." *Journal of Geotechnical Engineering*, ASCE, 122(5), 473-483.

Ou C.Y., Tang Y.G. (1994). "Soil parameter determination for deep excavation analysis by optimization." *Journal of the Chinese Institute of Engineering*, Vol. 17(5)}, pp.671-688

Peck R.B. (1969). "Deep excavations and tunneling in soft ground." *Proceedings, 7th International Conference of Soil mechanics and Foundation Engineering, State-of-the-ArtVolume*, 225-290.

Poeter EP and Hill M.C. (1997). "Inverse Methods: A Necessary Next Step in Groundwater Modeling," *Ground Water*, Vol. 35, no. 2, 250-260.

Poeter E.P. and Hill M.C. (1998). "Documentation of UCODE, a computer code for universal inverse modeling." U.S. *Geological Survey Water-Resources investigations report 98-4080*, 116 pp.

Sakurai S. and Takeuchi K. (1983). "Back analysis of measured displacements of tunnels," *Rock mechanics and rock engineering,* Vol.16, 173-180.

Santagata, M., Germaine, J.T. and Ladd, C.C. (2005). "Factors Affecting the Initial Stiffness of Cohesive Soils." *Journal of Geotechnical and Geoenvironmental Engineering*, ASCE, Vol. 131(4), 430-441.

Sabatini, P.J. (1991). "Sheet-pile installation effects on computed ground response for braced excavations in soft to medium clays." MS thesis, Northwestern University, Evanston, IL.

Schantz, T., Vermeer, P.A. and Bonnier, P.G. 1999. "Formulation and verification of the Hardening–Soil Model." *R.B.J. Brinkgreve, Beyond 2000 in Computational Geotechnics*. Balkema, Rotterdam, 281-290.

Stallebrass, S.E. and Taylor, R.N. (1997). "The development and evaluation of a constitutive model for the prediction of ground movements in overconsolidated clay." *Geotechnique*, Vol. 47 (2) 235-253.

Tu, X.X. (2007). "Tangent stiffness model for clays including small strain non-linearity." PhD thesis, Northwestern University, Evanston, IL.

Vorster, T.E.B., Mair, R.J., Soga, K., Klar, A. and Bennett, P.J. (2006). "Using BOTDR fibre optic sensors to monitor pipeline behaviour during tunnelling," Third European Workshop on Structural Health Monitoring, Granada

Viggiani, G. and Tamagnini, C. (1999). "Hypoplasticity for modeling soil non-linearity in excavation problems." *Pre-failure Deformation Characteristics of Geomaterials*, M. Jamiolkowski, M, Lancellotta, R. and Lo Presti, D. (eds.), Balkema, Rotterdam, 581-588.

Wakita, E. and Matsuo, M. (1994). "Observational design method for earth structures constructed on soft ground." *Géotechnique*. 44, No. 4, 747-755.

Whittle, A.J. and Kavvadas, M.J. (1994). "Formulation of MIT-E3 constitutive model for overconsolidated clays." *Journal of Geotechnical and Geoenvironmental Engineering*, ASCE, Vol. 120(1), 173-198.

Yamagami T., Jiang J.C., Ueta, Y. (1997). "Back calculation of strength parameters for landslide control works using neural networks." *Proceedings of the 9th Int. Conf. on Computer Methods and Advances in Geomechanics*, Wuhan, China.